Year: 2008

Paradoxical effects of increased expression of PGC-1α on muscle mitochondrial function and insulin-stimulated muscle glucose metabolism

Choi, C. S. and Befroy, D. E. and Codella, R. and Kim, S. and Reznick, R. M. and Hwang, Y. -J. and Liu, Z. -X. and Lee, H. -Y. and Distefano, A. and Samuel, V. T. and Zhang, D. and Cline, G. W. and Handschin, C. and Lin, J. and Petersen, K. F. and Spiegelman, B. M. and Shulman, G. I.

Originally published as:

Choi, C. S. and Befroy, D. E. and Codella, R. and Kim, S. and Reznick, R. M. and Hwang, Y. -J. and Liu, Z. -X. and Lee, H. -Y. and Distefano, A. and Samuel, V. T. and Zhang, D. and Cline, G. W. and Handschin, C. and Lin, J. and Petersen, K. F. and Spiegelman, B. M. and Shulman, G. I.. (2008) Paradoxical effects of increased expression of PGC-1α on muscle mitochondrial function and insulin-stimulated muscle glucose metabolism. Proceedings of the National Academy of Sciences of the United States of America, Vol. 105, H. 50. S. 19926-19931.

Paradoxical Effects of Increased Expression of PGC-1α on Muscle Mitochondrial Function and Insulin Stimulated Muscle Glucose Metabolism

Cheol Soo Choi*[1,5], Douglas E. Befroy*[1], Roberto Codella*[1], Sheene Kim[1], Richard M. Reznick[1], Yu-Jin Hwang[1], Zhen-Xiang Liu[1], Hui-Young Lee[1], Alberto Distefano[1], Varman T. Samuel[1], Dongyan Zhang[1], Gary W. Cline[1], Christoph Handschin[4], Jiandie Lin[4], Kitt F. Petersen[1], Bruce M. Spiegelman[4] and Gerald I. Shulman[1,2,3]

[1]Departments of Internal Medicine, [2]Cellular & Molecular Physiology and [3]Howard Hughes Medical Institute, Yale University School of Medicine, New Haven, CT 06510; [4]Department of Cell Biology, Dana Farber Cancer Institute, Harvard Medical School, Boston, MA; [5]Lee Gil Ya Cancer and Diabetes Institute, Gachon University of Medicine and Science, Korea

Published in Proc Natl Acad Sci U S A. 2008 Dec 16;105(50):19926-31. PMID: 19066218. doi: 10.1073/pnas.0810339105.

Biological Sciences: Medical Sciences

Paradoxical Effects of Increased Expression of PGC-1α on Muscle Mitochondrial Function and Insulin Stimulated Muscle Glucose Metabolism

Cheol Soo Choi*[1,5], Douglas E. Befroy*[1], Roberto Codella*[1], Sheene Kim[1], Richard M. Reznick[1], Yu-Jin Hwang[1], Zhen-Xiang Liu[1], Hui-Young Lee[1], Alberto Distefano[1], Varman T. Samuel[1], Dongyan Zhang[1], Gary W. Cline[1], Christoph Handschin[4], Jiandie Lin[4], Kitt F. Petersen[1], Bruce M. Spiegelman[4] and Gerald I. Shulman[1,2,3]

[1]Departments of Internal Medicine, [2]Cellular & Molecular Physiology and [3]Howard Hughes Medical Institute, Yale University School of Medicine, New Haven, CT 06510; [4]Department of Cell Biology, Dana Farber Cancer Institute, Harvard Medical School, Boston, MA; [5]Lee Gil Ya Cancer and Diabetes Institute, Gachon University of Medicine and Science, Korea

* The authors contributed equally towards this manuscript.

Address correspondence to:
Gerald I. Shulman, M.D., PhD.
TAC S269, PO Box 9812
Yale University School of Medicine, New Haven, CT 06536-8012
Phone: (203) 785-5447, Fax: (203) 737-4059
E-mail: gerald.shulman@yale.edu

Manuscript information:

- **Number of text pages: 20**
- **Number of figures: 6**
- **Number of tables: 2**

Abbreviations footnote: Acc, acetyl coenzyme A carboxylase; CPT1, carnitine palmitoyl transferase 1; CoA, coenzyme A; EDL, extensor digitorum longus**;** MRS, magnetic resonance spectroscopy; PKC, protein kinase C;
Conflict of interest: The authors declare no conflict of interest.

Author contributions: C.S.C., D.E.B., R.C., S.K., R.M.R., Y.H. and G.I.S. designed the research protocols; C.S.C., D.E.B., S.K., R.M.R, Y.H., Z.L., A.D., V.T.S., and R.C. performed the research; C.S.C., D.E.B., S.K., R.M.R, Y.H., Z.L., A.D., V.T.S., R.C., G.W.C., C.H., J.L., K.F.P., B.M.S. and G.I.S. analyzed data and contributed to the writing of this manuscript.

ABSTRACT

Peroxisome proliferator–activated receptor-γ coactivator (PGC)-1α has been shown to play critical roles in regulating mitochondrial biogenesis, respiration, and muscle oxidative phenotype. Furthermore reductions in the expression of PGC-1α in muscle have been implicated in the pathogenesis of type 2 diabetes. To determine the effect of increased muscle specific PGC-1α expression on muscle mitochondrial function and glucose and lipid metabolism *in vivo*, we examined body composition, energy balance, liver and muscle insulin sensitivity by hyperinsulinemic-euglycemic clamp studies, and muscle energetics using ^{31}P Magnetic Resonance Spectroscopy in transgenic mice. Increased expression of PGC-1α in muscle resulted in a 2.4 fold increase in mitochondrial density, which was associated with an ~60% increase in the unidirectional rate of ATP synthesis. Surprisingly, there was no effect of increased muscle PGC-1α expression on whole body energy expenditure and PGC-1α TG mice were more prone to fat-induced insulin resistance due to decreased insulin-stimulated muscle glucose uptake. The reduced insulin-stimulated muscle glucose uptake could most likely be attributed to a relative increase in fatty acid delivery/triglyceride reesterfication, as reflected by increased expression of CD36, DGAT1 and mtGPAT, that may have exceeded mitochondrial fatty acid oxidation resulting in increased intracellular lipid accumulation and an increase in the membrane to cytosol diacylglycerol content. This in turn caused activation of PKCθ, decreased insulin signalling at the level of IRS-1 tyrosine phosphorylation and skeletal muscle insulin resistance.

\body

Introduction

Type 2 diabetes is the most common metabolic disease in the world and although the primary cause of this disease is unknown, it is clear that insulin resistance plays an early and critical role in its pathogenesis (1-3). Many studies suggest that net lipid accumulation (4-6), due to an imbalance between fatty acid delivery/synthesis and fatty acid oxidation, results in activation of a serine kinase cascade. This in turn inhibits insulin signalling resulting in insulin resistance in liver and skeletal muscle, the organs responsible for the majority of glucose disposal. Studies in transgenic and knockout mice have demonstrated that alterations in fatty acid delivery (5, 7), synthesis (8) or mitochondrial (9-11)/peroxisomal (12) fatty acid oxidation can alter this balance resulting in insulin resistance when there is a net increase in intracellular diacylglycerol content and protection from insulin resistance when there is a net reduction in intracellular diacylglycerol content.

Peroxisome proliferator–activated receptor-γ coactivator (PGC-1α) is a critical regulator of mitochondrial biogenesis in skeletal muscle and promotes this process in response to exercise to maintain a balance between energy need and energy supply (13, 14). Furthermore, two recent microarray studies have implicated decreased PGC-1α expression and reduction in the expression of OXPHOS genes encoded by PGC-1α in the pathogenesis of type 2 diabetes mellitus (15, 16). Therefore, we hypothesized that increased expression of PGC-1α would prevent against fat induced insulin resistance. Given the important role of PGC-1α in stimulating mitochondrial biogenesis and potentially affecting the balance between fatty acid delivery/synthesis versus fatty acid oxidation in muscle, we decided to examine the impact of

increased PGC-1α expression on *in vivo* muscle mitochondrial function and glucose and lipid metabolism in muscle specific PGC-1α transgenic mice fed a high fat diet.

Results

Increased expression of PGC-1α in muscle elevated mitochondrial density and OXPHOS genes.

MCK-PGC-1α transgenic (MPGC-1α TG) mice had an ~6 fold increase in gene expression of PGC-1α (Figure 1A) and 2.4 fold higher mitochondrial density in the extensor digitorum longus muscle (EDL, mainly type II fibers), assessed by electron microscopy, as compared with WT mice (Figure 1B). The expression of a number of OXPHOS and mitochondrial genes was significantly increased including subunits of NADH-ubiquinone oxidoreductase (Ndufs1 and Ndufv2), cytochrome c (Cycs), cytochrome c oxidase (Cox5b) and ATP synthase (APT5o), which have been shown to be directly regulated by PGC-1α (Figure 1C). However, there was no difference in mitochondrial density in soleus muscle (type I fiber muscle, data not shown), which indicates that increased expression of PGC-1α was predominant in type II fibers of MPGC-1α TG mice due to preferential expression of the MCK promoter in this fiber-type.

Increased expression of PGC-1α in muscle did not change fat mass or energy expenditure.

Total body weight, fat mass and lean body mass were similar between MPGC-1α TG and WT littermate mice fed a regular diet. High fat feeding for 3 weeks increased fat mass in MPGC-1α TG to the same extent as in WT littermates (Table 1). To assess energy balance, mice were housed in metabolic cages for 4 days (2 day acclimation followed by 2 day study). Consistent with the effects on body weight change, no differences in food intake, activity and total energy expenditure were observed between MPGC-1α TG and WT mice fed either regular chow or high fat diet (Table 1). The respiratory quotient (RQ), which represents substrate preference as fuel, indicated that whole body fat oxidation was unaffected in MPGC-1α TG fed a regular-chow

[carbohydrate rich (12% fat)] diet. Switching WT mice to a high-fat diet (55% fat) significantly increased fat oxidation (reduced RQ) in the fed state, whereas altering the diet failed to increase fat oxidation any further in MPGC-1α TG mice. These data demonstrate that increased PGC-1α gene expression and mitochondrial density in skeletal muscle does not alter whole body energy expenditure, body weight or fat mass.

Insulin sensitivity was paradoxically decreased in MPGC-1α TG mice fed a high-fat diet.

Fasting plasma glucose and insulin concentrations were similar between the two groups, fed either the regular or high-fat diet (Table 2). Plasma lipid profiles, including plasma fatty acids, triglycerides and cholesterol were similar under fasting and insulin-stimulated conditions in both groups fed either regular or high-fat diet (Table 2). No difference in insulin sensitivity, assessed by the hyperinsulinemic-euglycemic clamp, was observed in the two groups of mice when fed a regular diet (data not shown). In contrast, MPGC-1α TG mice were insulin resistant compared to WT control mice when fed a high-fat fed diet, reflected by a 60% reduction in the glucose infusion rate required to maintain euglycemia during the clamp (Figure 2A). The whole body insulin resistance could be mostly attributed to a 25% reduction in insulin-stimulated whole body glucose uptake and a 56% reduction in whole body glycogen synthesis (Figure 2C). There were no differences in basal or insulin mediated suppression of hepatic glucose production between the groups (Figure 2B). Consistent with the peripheral insulin resistance observed during the clamp, 2-deoxy-glucose uptake was decreased by 60% in MPGC-1α TG mice, compared with WT mice (Figure 2D). These changes were associated with a reduction in insulin-stimulated IRS1 tyrosine phosphorylation and Akt2 activity (Figure 2E, F).

Mechanism for increased insulin resistance in skeletal muscle in PGC-1α TG mice.

Consistent with our hypothesis of lipid metabolites inducing insulin resistance (6, 9, 10, 17-20), muscle triglyceride, lysophosphatidic acid and long chain acyl CoAs were markedly increased in MPGC-1α TG mice fed a high fat diet, compared with WT mice (Figure 3A, C, D). The membrane/cytosol ratio of skeletal muscle diacylglycerol, a known activator of PKCs, was increased by ~50% in the MPGC-1α TG mice compared to WT mice (Figure 3B) and was associated with a 40% increase in PKCθ activity, as reflected by an increase in PKCθ translocation from cytosol to membrane (Figure 3E).

A recent study suggested that PGC-1α induces insulin resistance in liver through peroxisome proliferator–activated receptor (PPAR)-α dependent induction of mammalian tribbles homolog (TRB-3), which has been suggested to be a direct negative regulator of AKT activity in some (21, 22), but not all studies (23, 24). Since overexpression of PGC-1α was also found to significantly increase TRB-3 expression in skeletal muscle (25) we examined TRB-3 gene expression in muscle of MPGC-1α TG mice. TRB-3 mRNA and protein levels were approximately twofold increased in MPGC-1α TG mice, compared with WT mice (Figure 4A, B).

Muscle oxidative function *in vivo* and *ex vivo*.

Net intracellular lipid accumulation in skeletal muscle can occur as a result of increased fatty acid delivery/synthesis and/or reduced fatty acid oxidation. To estimate mitochondrial function *in vivo* we used ^{31}P saturation-transfer MRS to assess the unidirectional rate of muscle ATP synthesis (V_{ATP}) (33, 35). Skeletal muscle V_{ATP} was increased by 50-60% in the hindlimb of MPGC-1α TG mice fed either regular or high-fat diet compared to the WT mice (Figures 5A, B).

In addition, the ratio of inorganic phosphate to phosphocreatine was increased by 53% in MPGC-1α TG mice fed HFD compared to WT mice (0.236 ± 0.01 vs. 0.154 ± 0.01, P< 0.001), which may reflect a higher ratio of type I fibers (mostly oxidative) to type II fibers (mostly glycolytic) (27). Rates of fat oxidation measured *ex vivo* in isolated muscle strips, were increased by 30% in the EDL (predominantly type IIb muscle fibers) of MPGC-1α TG mice compared to WT mice, but were unaltered in soleus muscle (mainly type I muscle fibers) (Figures 5 C, D).

Gene expression involved in fatty acid oxidation and uptake.

Consistent with effects on muscle oxidative function, the expression of several oxidative/thermogenic genes (*CPT1, CPT2, VLCAD, LCAD, MCAD* and *UCP2*) and of CPT1 protein were increased in the tibialis anterior muscle (predominantly type II muscle fibers) of MPGC-1α TG mice with respect to WT mice (Figure 5E, F). In addition, gene and protein expression of ACC2 was increased and the phospho-ACC2 level was also increased in MPGC-1α TG mice compared to WT mice (Figure 5E, F). However, there was no difference in AMPK-α2 activity in the EDL muscle, between the two groups [WT (n=6) vs.TG mice (n=6): 0.63 ± 0.08 vs. 0.58 ± 0.18 pmol/min/mg, NS]. There was a marked increase in the expression of genes of fatty acid transport (*CD36*) and fatty acid reesterification (*mtGPAT and DGAT1*) in skeletal muscle of the MPGC-1α TG mice compared to the WT mice (Figure 6).

Discussion

Given the important role that muscle mitochondria play in whole body glucose and fat metabolism we sought to examine the impact of increased mitochondrial content on oxidative metabolism and fat-induced insulin resistance in transgenic mice with increased expression of PGC-1α in skeletal muscle. We found that the increased mitochondrial content in these transgenic mice was accompanied by increased oxidative metabolism measured both *in vivo* and *ex vivo*, however this did not prevent diet-induced obesity. Furthermore, MPGC-1α TG mice were more prone to fat-induced muscle insulin resistance, which could be attributed to reduced insulin-stimulated glucose uptake in skeletal muscle.

These results are contrary to previous studies that found increased glucose uptake in both C2C12 and L6 muscle cells that overexpressed PGC-1α (28) and *ex vivo* muscle with electrotransfection of PGC-1α (29). It is possible that the differences in these results may be due to the relatively higher expression of PGC-1α in the transgenic mice compared to the *in vitro* studies. However, it should be noted that the increased expression of PGC-1α in muscles composed of type II fibers was approximately 6 fold, which is well within the 10-13 fold increase observed following exercise training, and similar to that found in type I muscle fibers (30). Moreover, in contrast to the current *in vivo* studies, insulin sensitivity under conditions of increased fatty acid exposure was not tested in these *in vitro* cultured cell and *ex vivo* muscle studies (28, 29).

To understand the mechanism for the reduced insulin-stimulated glucose uptake in skeletal muscle in the MPGC-1α TG mice we examined the insulin signaling pathway and found that both insulin-stimulated IRS-1 tyrosine phosphorylation and insulin-stimulated AKT2 activity were significantly reduced in skeletal muscle. In addition, we found that the expression

of TRB-3, a mammalian homolog of Drosophila tribble, which has recently been suggested by some (21, 22) but not all studies (23, 24) to be a direct negative regulator of AKT activity, was increased by approximately twofold in skeletal muscle of the PGC-1α TG mice, consistent with previous observations (25). However, given the controversy regarding the role of TRB-3 in causing insulin resistance, further studies will be necessary to determine if increased TRB- expression contributes to the observed insulin resistance in MPGC-1α TG mice. Furthermore, since TRB-3 has been implicated to cause insulin resistance at the level of AKT2 it cannot explain the reduced insulin-stimulated IRS-1 tyrosine phosphorylation. Previous studies have implicated that increases in intracellular diacylglycerol, due to an imbalance between fatty acid delivery/synthesis and fatty acid oxidation, results in activation of PKCθ which reduces insulin signaling at the level of the insulin receptor and IRS-1 tyrosine phosphorylation in muscle (6, 17). Consistent with this hypothesis, we observed increases in the membrane/cytosol ratio of diacylglycerol, associated with increased activation of PKCθ in the MPGC-1α TG mice.

This was an unexpected result given the twofold increase in mitochondrial content. To determine whether the mitochondria were dysfunctional we examined a biomarker of *in vivo* mitochondrial function in the MPGC-1α TG mice with ^{31}P saturation-transfer MRS (*26*). Using this approach we found that mitochondrial ATP synthesis per gram muscle was increased by 60% in the MPGC-1α TG mice. This was somewhat less than the 2.4 fold increase in mitochondrial density, suggesting partial downregulation of activity per unit of mitochondrial mass in the MPGC-1α TG mice. However, the mechanism responsible for this effect remains to be determined. Despite increased muscle ATP production *in vivo*, and enhanced fat oxidation *ex vivo*, in MPGC-1α TG mice, no effects on whole body energy expenditure could be detected. Potentially, these mice could have enhanced mitochondrial coupling of oxidative

phosphorylation (an elevated P:O ratio). We have estimated the efficiency of mitochondrial energy production, *in vivo,* in a variety of human and animal models using MRS biomarkers of mitochondrial metabolism and have found that the P:O ratio is unaffected (26, 31) unless mitochondrial coupling is deliberately targeted (e.g. by T_3 and 2,4 dinitrophenol treatment) or by modulating uncoupling protein expression (32-34). More recently, we have observed that endurance trained human muscle, likely to have an increased mitochondrial content, is actually less well coupled under resting conditions (35). Therefore, we believe that modulation of the P:O ratio is unlikely to cause the effects observed in these mice. A more likely explanation is that the measurement of whole body energy expenditure is not sensitive enough to detect an increase in muscle ATP production.

Given the significant increase in intramuscular triglyceride and fat metabolites in the MPGC-1α. TG mice, despite a concomitant increase in mitochondrial function and fatty acid oxidation, we investigated whether this could be attributed to increased fatty acid delivery and/or fat synthesis in the skeletal muscle of these mice. Consistent with this hypothesis we found that gene expression for *CD36*, a key fatty acid transporter, and *mtGPAT and DGAT1,* two key rate controlling enzymes for triglyceride reesterification, were markedly increased in the muscle of the MPGC-1α TG mice. It has been demonstrated that PGC-1α coactivates PPARs and the promoter of CD36 has a PPAR response element sequence (36), therefore increased expression of PGC-1α could result in enhanced CD36 expression and increased uptake of fatty acids. However, the mechanism by which increased PGC-1α expression elevates the gene expression of *mtGPAT* and *DGAT1* is less clear. PGC-1α, in contrast to PGC-1β, is not known to regulate SREBP1c activity (37), although it is possible that interactions via LXR could affect these genes (37, 38).

Taken together these data are consistent with the hypothesis that under normal physiologic conditions of exercise, PGC-1α induces a coordinated program of increased energy delivery and increased mitochondrial biogenesis and fatty acid oxidation to meet the increased energy demands of working skeletal muscle. In contrast, this same coordinated program, in the non exercising MPGC-1α TG mice, results in a mismatch between increased fatty acid uptake and that of mitochondrial fat oxidation resulting in a net increase intramyocellular fat and diacylglycerol content and insulin resistance. Recently Koves et al. have proposed that fat-induced insulin resistance in muscle might also arise from increased fatty acid transport into mitochondria resulting in incomplete β-oxidation (39). Further studies will be necessary to determine if this mechanism is also contributing to skeletal muscle insulin resistance in this mouse model.

In summary, we have shown that increased muscle expression of PGC-1α paradoxically exacerbated fat-induced insulin resistance in skeletal muscle despite an increase in mitochondrial density and mitochondrial activity. This insulin resistance could be attributed to net increases in the membrane/cytosol diacylglycerol content, due to relative increases in fatty acid uptake and reesterification exceeding mitochondrial fatty acid oxidation. The increase in membrane/cytosol diacylglycerol content in turn leads to activation of PKCθ and decreased insulin signalling at the level of IRS-1 tyrosine phosphorylation and results in insulin resistance in skeletal muscle.

Materials and Methods

Animals. MPGC-1α TG mice were generated as previously described (40). PGC-1α complementary DNA was placed downstream of a 6.5-kilobase (kb) MCK promoter sequence. MPGC-1α TG mice were generated by standard DNA microinjection and identified by PCR-based genotyping. Male MPGC-1α TG mice and littermates (12-14 weeks of age) were studied under controlled temperature (22±2oC) and lighting (12-h light; 0700-1700 h, 12-h dark; 1700-0700 h). To examine diet-induced changes in glucose and fat metabolism, male MPGC-1α TG and WT mice were fed with high-fat diet (55% fat by calories; Harlan Teklad, Madison, WI) ad libitum for 3 weeks. All mice were maintained in accordance with the institutional Animal Use and Care Committee of Yale University School of Medicine.

Basal metabolic parameters. Fat and lean body masses were assessed by a ^{1}H minispec system (Bruker BioSpin, Billerica, MA) before and after 3 week's high fat feeding. Activity, food consumption, and energy expenditure were evaluated before and after 3 weeks of high fat feeding (CLAMS: Columbus instruments, Columbus, OH, USA) as previously described (10).

Hyperinsulinemic-euglycemic clamp study. After an overnight fast, hyperinsulinemic-euglycemic clamp was conducted for 120 min with a primed/continuous infusion of human insulin (126 pmol/kg prime, 18 pmol/kg/min infusion) (Novo Nordisk, Princeton, NJ) as previously described (10). During the clamp, plasma glucose was maintained at basal concentrations (~6.7 mM). Rates of basal and insulin-stimulated whole-body glucose fluxes and tissue glucose uptake were determined as previously described (10).

Biochemical Analysis. Plasma glucose and insulin were determined by a glucose oxidase method (Beckman glucose analyzer II, Beckman, Fullerton, CA) and radioimmunoassay (RIA kit from Linco Research, St. Louis, MO, U.S.A.). Plasma FFA was determined using an acyl-CoA

oxidase based colorimetric kit (Wako Pure Chemical Industries, Osaka, Japan). Plasma resistin, leptin, TNFα and IL-6 were measured by multiplexed biomarker immunoassays (Lincoplex) from Linco Research (St. Charles, MO, U.S.A.).

Insulin signaling and PKCθ. IRS1 tyrosine phosphorylation and Akt2 activity were assessed in protein extracts from muscle harvested after short-term insulin stimulation as previously described (10). Primary antibodies used for experiments were rabbit polyclonal IgG: Antibodies for IRS1 tyrosine phosphorylation and Akt2 were obtained from Upstate (Charlottesville, Virginia, USA). PKCθ membrane translocation assay was conducted as previously described (10). Membrane translocation of PKCθ was expressed as the ratio of membrane bands over cytosol bands (arbitrary units).

Total RNA preparation, real-time quantitative RT-PCR analysis and immunoblotting analysis. Total RNA was isolated from tibialis anterior muscle of the mice fed regular diet using total RNA isolation reagent (BL-10500, Biotecx Laboratories Inc.). Quantitative RT-PCR was performed using custom-made RT-PCR enzymes and reagents kit (Invitrogen Life Technology Inc.) and ABI Prism 7700 Sequence Detector (PE Applied Biosciences). For Western protein analysis, forty micrograms of cell lysates were separated on 4-12% SDS-PAGE and immunoblotted with TRB3 (provided by Marc Montminy), CPT1 (Santa Cruz biotechnology), ACC2 (Santa Cruz biotechnology) or anti-p-ACC 2 (Ser219/221, Santa Cruz biotechnology) antibodies.

AMPK activity assays: The EDL muscle was quickly freeze-clamped in situ and kept in liquid nitrogen until analyzed. AMPK activity was assessed previously described (41). Muscles were ground and mixed with 1 ml of lysis buffer. Homogenates were spun at 20,800 × g for 10 min at 4°C, and protein concentrations were determined. AMPK-α_2 was immunoprecipitated overnight

from cell lysates containing 1 mg of protein using 1 μl of AMPK-α_2 antibody (Santa Cruz Biotechnology). Skeletal muscle AMPK-α_2 activity was determined by following the incorporation of [^{32}P]ATP into a synthetic peptide containing the AMARA sequence on the following day.

Transmission electron microscopy analysis. Mitochondrial density was assessed by a Tecnai 12 BiolTWIN electron microscopy (FEI Co.) in soleus and EDL muscle as previously described (18). For each set of 5 pictures from 3 random sections of individual muscle, average volume density was calculated and the mean of 3 values used to estimate the volume density for each muscle.

Tissue lipid measurement. Intracellular fatty acid metabolites, such as lysophosphatidic acid and long-chain fatty acyl-CoAs were measured by using an API 4000 tandem mass spectrometer (Applied Biosystems) in conjunction with two Perkin Elmer 200 Series micro pumps and a 200 Series autosampler (Perkin Elmer) (8). To determine the level of diacylglycerol in cytosol and membrane, diacylglycerol extraction and analysis in both cytosolic and membrane samples was performed as previously described (8, 19). Tissue triglyceride was extracted using the method of Bligh and Dyer (42) and measured using a DCL Triglyceride Reagent (Diagnostic Chemicals Ltd.).

Skeletal muscle fatty acid oxidation rate. Skeletal muscle (about 10~15 mg of soleus and EDL muscles) was quickly removed from mice and muscle fatty acid oxidation was assessed with trapping $^{14}CO_2$ after incubation with albumin bound 2uCi of [1-^{14}C] oleic acid (43).

Unidirectional rate of muscle ATP synthesis by *in vivo* ^{31}P-MRS. The unidirectional rate of muscle ATP synthesis (V_{ATP}) was assessed by ^{31}P saturation-transfer MRS using a 9.4 T superconducting magnet (Magnex Scientific, UK) interfaced to a Bruker Biospec console. After

an overnight fast, the mouse was sedated using ~1% isoflurane and the left hindlimb was positioned under a 15mm diameter ^{31}P surface coil. Non-localized ^{31}P saturation-transfer spectra were acquired with saturation of the γ-ATP resonance or at a downfield frequency equidistant from the Pi resonance (control saturation) using the following parameters: 1ms AHP excitation pulse (centered between Pi and γ-ATP) 10s frequency-selective saturation pulse, sweep width = 8 kHz, 1024 complex points, effective T_R = 10s, 64 averages. Fully-relaxed ^{31}P spectra (T_R = 25 sec, 32 averages) were also obtained to determine metabolite concentrations. The T_1 of P_i under γ-ATP saturation (T_1') was measured using an 8-point inversion-recovery sequence (2ms AFP inversion pulse) with γ-ATP-saturation prior to and during the inversion delay. All MR data was processed using XWINNMR (version 6.5; Bruker Biospin, Germany); prior to Fourier transformation ^{31}P FIDs were zero-filled to 32k points and multiplied by a mixed Lorentzian / Gaussian function (lb -20/ gb 0.04). ^{31}P spectra were baseline corrected by fitting to a 5th order polynomial. The unidirectional rate of $P_i \rightarrow$ ATP flux was determined as previously described (33, 35).

Statistics

All results are expressed as means ± SEM of 'n' observations. Statistical differences between the means were assessed by a 2-tailed Student's t-test, $^{*}P < 0.05$.

Acknowledgements

We thank Mario Kahn and Xiaoxian Ma for expert technical assistance with the studies. This work was supported by grants from the United States Public Health Services, R01 DK-40936, U24 DK-76169 and P30 DK-45735 (to G.I.S.). G. I. Shulman is an investigator of The Howard Hughes Medical Institute and the recipient of a Distinguished Clinical Investigator Award from the American Diabetes Association.

References

1. Zimmet P, Alberti KG, & Shaw J (2001) Global and societal implications of the diabetes epidemic. *Nature* 414(6865):782-787.
2. Lillioja S, *et al.* (1993) Insulin resistance and insulin secretory dysfunction as precursors of non-insulin-dependent diabetes mellitus. Prospective studies of Pima Indians. *N Engl J Med* 329(27):1988-1992.
3. DeFronzo RA, Bonadonna RC, & Ferrannini E (1992) Pathogenesis of NIDDM. A balanced overview. *Diabetes Care* 15(3):318-368.
4. Boden G & Shulman GI (2002) Free fatty acids in obesity and type 2 diabetes: defining their role in the development of insulin resistance and beta-cell dysfunction. *Eur J Clin Invest* 32 Suppl 3:14-23.
5. Kim JK, *et al.* (2001) Tissue-specific overexpression of lipoprotein lipase causes tissue-specific insulin resistance. *Proc Natl Acad Sci U S A* 98(13):7522-7527.
6. Shulman GI (2000) Cellular mechanisms of insulin resistance. *J Clin Invest* 106(2):171-176.
7. Kim JK, *et al.* (2004) Inactivation of fatty acid transport protein 1 prevents fat-induced insulin resistance in skeletal muscle. *J Clin Invest* 113(5):756-763.
8. Neschen S, *et al.* (2005) Prevention of hepatic steatosis and hepatic insulin resistance in mitochondrial acyl-CoA:glycerol-sn-3-phosphate acyltransferase 1 knockout mice. *Cell Metab* 2(1):55-65.
9. Choi CS, *et al.* (2007) Overexpression of uncoupling protein 3 in skeletal muscle protects against fat-induced insulin resistance. *J Clin Invest* 117(7):1995-2003.
10. Choi CS, *et al.* (2007) Continuous fat oxidation in acetyl-CoA carboxylase 2 knockout mice increases total energy expenditure, reduces fat mass, and improves insulin sensitivity. *Proc Natl Acad Sci U S A* 104(42):16480-16485.
11. Zhang D, *et al.* (2007) Mitochondrial dysfunction due to long-chain Acyl-CoA dehydrogenase deficiency causes hepatic steatosis and hepatic insulin resistance. *Proc Natl Acad Sci U S A* 104(43):17075-17080.
12. Neschen S, *et al.* (2007) n-3 Fatty acids preserve insulin sensitivity in vivo in a peroxisome proliferator-activated receptor-alpha-dependent manner. *Diabetes* 56(4):1034-1041.
13. Puigserver P, *et al.* (1999) Activation of PPARgamma coactivator-1 through transcription factor docking. *Science* 286(5443):1368-1371.
14. Wu Z, *et al.* (1999) Mechanisms controlling mitochondrial biogenesis and respiration through the thermogenic coactivator PGC-1. *Cell* 98(1):115-124.
15. Mootha VK, *et al.* (2003) PGC-1alpha-responsive genes involved in oxidative phosphorylation are coordinately downregulated in human diabetes. *Nat Genet* 34(3):267-273.
16. Patti ME, *et al.* (2003) Coordinated reduction of genes of oxidative metabolism in humans with insulin resistance and diabetes: Potential role of PGC1 and NRF1. *Proc Natl Acad Sci U S A* 100(14):8466-8471.
17. Griffin ME, *et al.* (1999) Free fatty acid-induced insulin resistance is associated with activation of protein kinase C theta and alterations in the insulin signaling cascade. *Diabetes* 48(6):1270-1274.

18. Morino K, *et al.* (2005) Reduced mitochondrial density and increased IRS-1 serine phosphorylation in muscle of insulin-resistant offspring of type 2 diabetic parents. *J Clin Invest* 115(12):3587-3593.
19. Yu C, *et al.* (2002) Mechanism by which fatty acids inhibit insulin activation of insulin receptor substrate-1 (IRS-1)-associated phosphatidylinositol 3-kinase activity in muscle. *J Biol Chem* 277(52):50230-50236.
20. Kim JK, *et al.* (2004) PKC-theta knockout mice are protected from fat-induced insulin resistance. *J Clin Invest* 114(6):823-827.
21. Du K, Herzig S, Kulkarni RN, & Montminy M (2003) TRB3: a tribbles homolog that inhibits Akt/PKB activation by insulin in liver. *Science* 300(5625):1574-1577.
22. Koo SH, *et al.* (2004) PGC-1 promotes insulin resistance in liver through PPAR-alpha-dependent induction of TRB-3. *Nat Med* 10(5):530-534.
23. Iynedjian PB (2005) Lack of evidence for a role of TRB3/NIPK as an inhibitor of PKB-mediated insulin signalling in primary hepatocytes. *Biochem J* 386(Pt 1):113-118.
24. Okamoto H, *et al.* (2007) Genetic deletion of Trb3, the mammalian Drosophila tribbles homolog, displays normal hepatic insulin signaling and glucose homeostasis. *Diabetes* 56(5):1350-1356.
25. Mortensen OH, Frandsen L, Schjerling P, Nishimura E, & Grunnet N (2006) PGC-1alpha and PGC-1beta have both similar and distinct effects on myofiber switching toward an oxidative phenotype. *Am J Physiol Endocrinol Metab* 291(4):E807-816.
26. Petersen KF, *et al.* (2003) Mitochondrial dysfunction in the elderly: possible role in insulin resistance. *Science* 300(5622):1140-1142.
27. Kushmerick MJ, Moerland TS, & Wiseman RW (1992) Mammalian skeletal muscle fibers distinguished by contents of phosphocreatine, ATP, and Pi. *Proc Natl Acad Sci U S A* 89(16):7521-7525.
28. Michael LF, *et al.* (2001) Restoration of insulin-sensitive glucose transporter (GLUT4) gene expression in muscle cells by the transcriptional coactivator PGC-1. *Proc Natl Acad Sci U S A* 98(7):3820-3825.
29. Benton CR, *et al.* (2007) Modest PGC-1alpha overexpression in muscle in vivo is sufficient to increase insulin sensitivity and palmitate oxidation in SS, not IMF, mitochondria. *J Biol Chem*.
30. Miura S, Kai Y, Ono M, & Ezaki O (2003) Overexpression of peroxisome proliferator-activated receptor gamma coactivator-1alpha down-regulates GLUT4 mRNA in skeletal muscles. *J Biol Chem* 278(33):31385-31390.
31. Befroy DE, *et al.* (2007) Impaired mitochondrial substrate oxidation in muscle of insulin-resistant offspring of type 2 diabetic patients. *Diabetes* 56(5):1376-1381.
32. Lebon V, *et al.* (2001) Effect of triiodothyronine on mitochondrial energy coupling in human skeletal muscle. *J Clin Invest* 108(5):733-737.
33. Jucker BM, *et al.* (2000) Assessment of mitochondrial energy coupling in vivo by 13C/31P NMR. *Proc Natl Acad Sci U S A* 97(12):6880-6884.
34. Cline GW, *et al.* (2001) In vivo effects of uncoupling protein-3 gene disruption on mitochondrial energy metabolism. *J Biol Chem* 276(23):20240-20244.
35. Befroy D, *et al.* (2008 in press) Increased Substrate Oxidation and Mitochondrial Uncoupling in Skeletal Muscle of Endurance Trained Individuals. *Proc Natl Acad Sci U S A*.

36. Teboul L, *et al.* (2001) Structural and functional characterization of the mouse fatty acid translocase promoter: activation during adipose differentiation. *Biochem J* 360(Pt 2):305-312.
37. Lin J, *et al.* (2005) Hyperlipidemic effects of dietary saturated fats mediated through PGC-1beta coactivation of SREBP. *Cell* 120(2):261-273.
38. Oberkofler H, Schraml E, Krempler F, & Patsch W (2003) Potentiation of liver X receptor transcriptional activity by peroxisome-proliferator-activated receptor gamma co-activator 1 alpha. *Biochem J* 371(Pt 1):89-96.
39. Koves TR, *et al.* (2008) Mitochondrial overload and incomplete fatty acid oxidation contribute to skeletal muscle insulin resistance. *Cell Metab* 7(1):45-56.
40. Lin J, *et al.* (2002) Transcriptional co-activator PGC-1 alpha drives the formation of slow-twitch muscle fibres. *Nature* 418(6899):797-801.
41. Reznick RM, *et al.* (2007) Aging-associated reductions in AMP-activated protein kinase activity and mitochondrial biogenesis. *Cell Metab* 5(2):151-156.
42. Bligh EG & Dyer WJ (1959) A rapid method of total lipid extraction and purification. *Can J Biochem Physiol* 37(8):911-917.
43. Cha SH, Hu Z, Chohnan S, & Lane MD (2005) Inhibition of hypothalamic fatty acid synthase triggers rapid activation of fatty acid oxidation in skeletal muscle. *Proc Natl Acad Sci U S A* 102(41):14557-14562.

Table 1

Basal metabolic parameters of energy balance

Group	Regular diet		High fat diet	
	WT (n=8)	**MPGC-1α TG (n=8)**	**WT (n=8)**	**MPGC-1α TG (n=8)**
Body weight (g)	28.6 ± 0.4	28.2 ± 0.8	32.4 ± 0.7	32.3 ± 0.8
Fat mass (g)	1.91 ± 0.2	2.1 ± 0.3	5.64 ± 0.6	5.9 ± 0.5
Lean body mass (g)	22.2 ± 0.4	21.7 ± 0.7	22.3 ± 0.2	22.3 ± 0.4
Total Energy Expenditure (Kcal /h/Kg body mass)	16.0 ± 0.8	15.1 ± 0.8	16.5 ± 0.3	16.1 ± 0.9
Food intake (Kcal /h/Kg body mass)	18.3 ± 1.5	15.5 ± 1.6	19.7 ± 2.3	18.1 ± 2.6
Activity (count/h)	103.5 ± 26.3	111.0 ± 21.5	110.4 ± 19.7	81.1 ± 26.0
Respiratory quotient	0.929 ± 0.012	0.880 ± 0.023	0.840 ± 0.010	0.820 ± 0.010

Table 2

Plasma metabolite, hormone and cytokine data from high fat fed wild type and PGC-1α TG mice

	Regular diet				High fat diet			
Group	**Fast**		**Clamp**		**Fast**		**Clamp**	
	WT (n=9)	MPGC1α TG (n=9)	WT (n=9)	MPGC1α TG (n=9)	WT (n=7~9)	MPGC1α TG (n=7~9)	WT (n=9)	MPGC1α TG (n=6)
Glucose (mg/dl)	150 ± 11	142 ± 9	118 ± 3	114 ± 4	160 ± 7	164 ± 10	123 ± 3	119 ± 5
Insulin (μU/ml)	14.6 ± 1.7	13.4 ± 1.6	61.4 ± 5.8	63.1 ± 5.4	17.7 ± 1.6	20.3 ± 1.2	60.9 ± 5.2	73.3 ± 5.2
Fatty Acids (mEq/l)	0.98 ± 0.11	1.27 ± 0.13	0.58 ± 0.06	0.48 ± 0.09	0.98 ± 0.09	1.00 ± 0.04	0.90 ± 0.07	0.83 ± 0.06
Triglycerides (mg/dl)					69.5 ± 9.1	83.2 ± 7.9	nd	nd
Cholesterol (mg/dl)					91.1 ± 7.7	88.9 ± 2.5	nd	nd
β-hydroxbutarate (mM)					1.47 ± 0.25	0.9 ± 0.10†	nd	nd

nd: not determined.

Figure Legends

Figure 1. Increased expression of PGC-1α in muscle elevated mitochondrial density and OXPHOS genes. Total RNA was isolated from tibialis anterior muscle of the mice fed a regular diet (n = 5), PGC-1α (A) and OXPHOS gene (C) expression was assessed by realtime RT-PCR. Mitochondrial density was counted in the extensor digitorum longus muscle (n = 5), the arrow indicates a mitochondrion (B). APT5o, ATP synthase; Ndufs, NADH-ubiquinone oxidoreductase; Cycs, cytochrome c; Cox5b, cytochrome c oxidase;

Figure 2. Increased expression of PGC-1α in skeletal muscle paradoxically decreased peripheral insulin sensitivity in high-fat fed mice. Peripheral and hepatic insulin sensitivity was assessed by a hyperinsulinemic-euglycemic clamps **(A-D)**. **(A)** glucose infusion rates; **(B)** hepatic glucose production; **(C)** whole body glucose uptake, glycolysis and glycogen synthesis; (**D**) Skeletal muscle (gastrocnemius) glucose uptake. Consistent with decreased muscle insulin sensitivity, IRS1 tyrosine phosphorylation and AKT2 activity in skeletal muscle (gastrocnemius) were decreased in MPGC-1α TG compared to wild type mice (**E, F**). IRS1 tyrosine phosphorylation and Akt2 activity were assessed 14 minutes after an intraperitoneal insulin injection of 1 u/kg body weight. n = 6 – 8 per group.

Figure 3. Fat metabolites and membrane translocation of PKCθ were increased in skeletal muscle of MPGC-1α TG mice. Triglyceride (A), lysophosphatidic acid (C) and long chain acyl CoA (D) levels were significantly increased in muscle (gastrocnemius) in MPGC-1α TG mice. Membrane/cytosol ratio of diacylglycerol (B) and PKCθ (E) were significantly higher in muscle (gastrocnemius) of MPGC-1α TG mice compared with WT mice. n = 8 per group.

Figure 4. Increased expression of PGC-1α in muscle also elevated TRB-3 gene (n = 8) and protein expression (n = 4) in skeletal muscle. Total RNA was isolated from tibialis anterior muscle, TRB3 gene expression (A) was assessed by realtime RT-PCR, protein expression was confirmed by immunoblot (B).

Figure 5. In vivo rates of ATP production and ex vivo fat oxidation were increased in the muscle of increased PGC-1α expression. Saturation-transfer measurements of ATP synthesis rates (V_{ATP}) by ^{31}P-MRS in hind limb of mice (n = 6) on regular chow (**A**) and high fat diet (**B**). *Ex vivo* skeletal muscle fat oxidation rate in soleus muscle (**C**) and EDL muscle from mice (n = 6) fed a regular chow (**D**). The expression of oxidative/thermogenic genes in tibialis anterior muscle from mice (n = 5 - 6) fed regular chow assessed by realtime RT-PCR (**E**). Immunoblot analysis (n = 4) from selected genes for CPT1, ACC2 and phospho-ACC2 (Ser219/221) (**F**). PPARα, peroxisome proliferator activated receptor α; ACC2, acetyl coenzyme A carboxylase 2; CPT, carnitine palmitoyl transferase; VLCAD, very long-chain acyl-CoA dehydrogenase; LCAD, long-chain acyl-CoA dehydrogenase; MCAD, medium chain acyl-CoA dehydrogenase; UCP2, uncoupling protein 2.

Figure 6. The expression of the genes involved in fatty acid uptake and reesterification was increased in tibialis anterior muscle of MPGC-1α TG mice fed a regular chow (n = 5 - 6). LPL, lipoprotein lipase ; mtGPAT, mitochondrial acyl CoA: glycerol-sn-3-phosphate acyltransferase ; DGAT1, acyl coenzyme A (CoA): diacylglycerol acyltransferase1 ; SREBP1c, sterol-regulatory element binding protein 1c; LXRα, liver x receptor α;LXRβ, liver x receptor β

Table 1

Basal metabolic parameters of energy balance

Group	Regular diet		High fat diet	
	WT (n=8)	**MPGC-1α TG (n=8)**	**WT (n=8)**	**MPGC-1α TG (n=8)**
Body weight (g)	28.6 ± 0.4	28.2 ± 0.8	32.4 ± 0.7	32.3 ± 0.8
Fat mass (g)	1.91 ± 0.2	2.1 ± 0.3	5.64 ± 0.6	5.9 ± 0.5
Lean body mass (g)	22.2 ± 0.4	21.7 ± 0.7	22.3 ± 0.2	22.3 ± 0.4
Total Energy Expenditure (Kcal /h/Kg body mass)	16.0 ± 0.8	15.1 ± 0.8	16.5 ± 0.3	16.1 ± 0.9
Food intake (Kcal /h/Kg body mass)	18.3 ± 1.5	15.5 ± 1.6	19.7 ± 2.3	18.1 ± 2.6
Activity (count/h)	103.5 ± 26.3	111.0 ± 21.5	110.4 ± 19.7	81.1 ± 26.0
Respiratory quotient	0.929 ± 0.012	0.880 ± 0.023	0.840 ± 0.010	0.820 ± 0.010

Table 2

Plasma metabolite, hormone and cytokine data from high fat fed wild type and PGC-1α TG mice

	Regular diet				High fat diet			
Group	**Fast**		**Clamp**		**Fast**		**Clamp**	
	WT (n=9)	MPGC1α TG (n=9)	WT (n=9)	MPGC1α TG (n=9)	WT (n=7~9)	MPGC1α TG (n=7~9)	WT (n=9)	MPGC1α TG (n=6)
Glucose (mg/dl)	150 ± 11	142 ± 9	118 ± 3	114 ± 4	160 ± 7	164 ± 10	123 ± 3	119 ± 5
Insulin (μU/ml)	14.6 ± 1.7	13.4 ± 1.6	61.4 ± 5.8	63.1 ± 5.4	17.7 ± 1.6	20.3 ± 1.2	60.9 ± 5.2	73.3 ± 5.2
Fatty Acids (mEq/l)	0.98 ± 0.11	1.27 ± 0.13	0.58 ± 0.06	0.48 ± 0.09	0.98 ± 0.09	1.00 ± 0.04	0.90 ± 0.07	0.83 ± 0.06
Triglycerides (mg/dl)					69.5 ± 9.1	83.2 ± 7.9	nd	nd
Cholesterol (mg/dl)					91.1 ± 7.7	88.9 ± 2.5	nd	nd
β-hydroxbutarate (mM)					1.47 ± 0.25	0.9 ± 0.10†	nd	nd

nd: not determined.

Figure 1

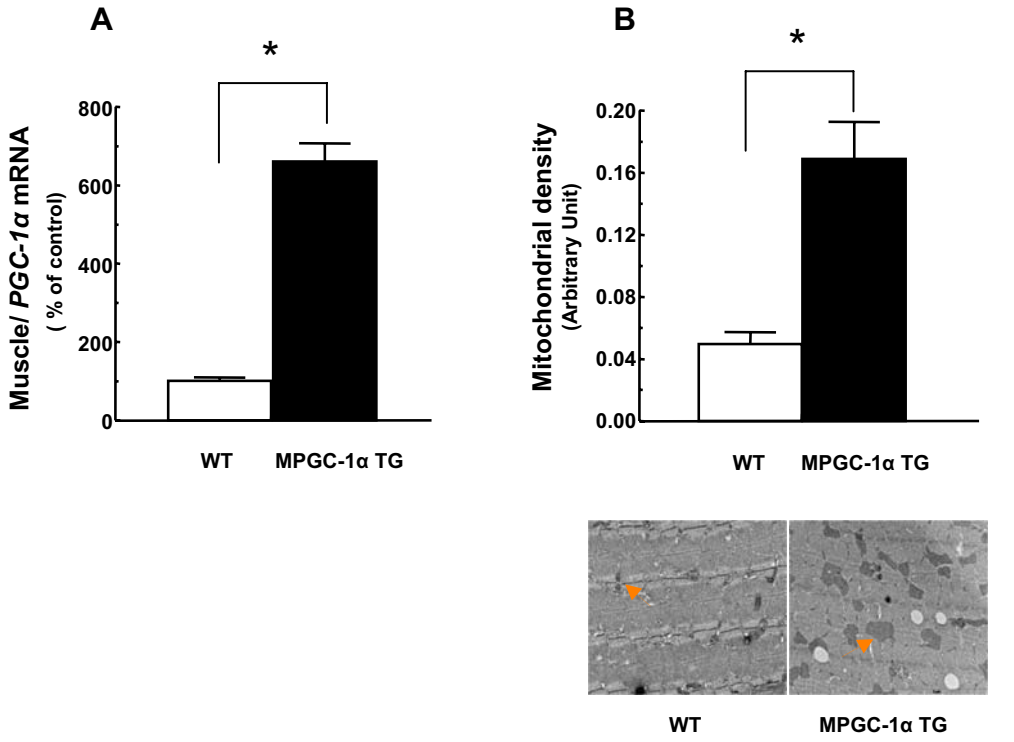
A
*
Muscle/ PGC-1α mRNA
(% of control)
800
600
400
200
0
WT
MPGC-1α TG
B
*
Mitochondrial density
(Arbitrary Unit)
0.20
0.16
0.12
0.08
0.04
0.00
WT
MPGC-1α TG
WT
MPGC-1α TG

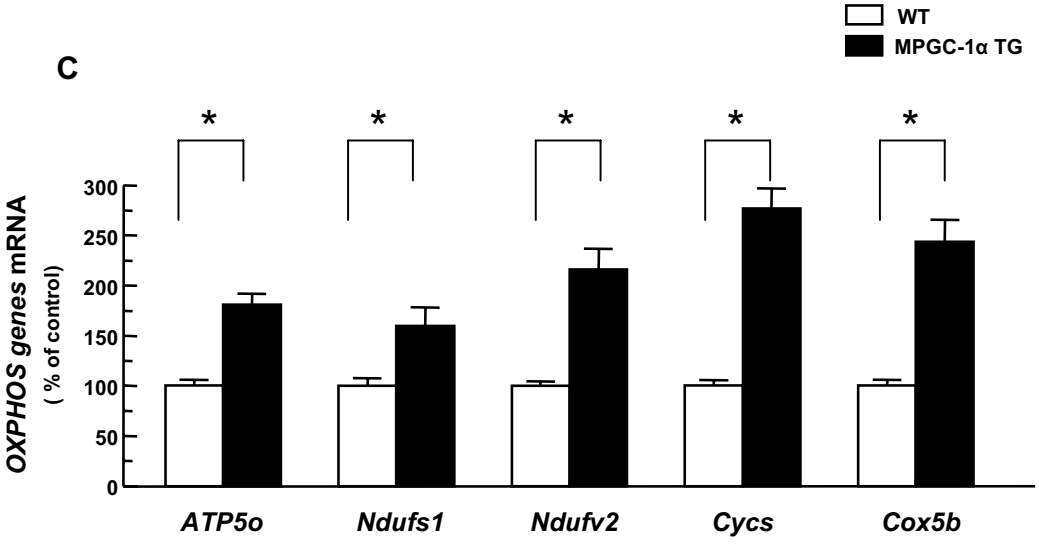
C
WT
MPGC-1α TG
*
*
*
*
*
OXPHOS genes mRNA
(% of control)
300
250
200
150
100
50
0
ATP5o
Ndufs1
Ndufv2
Cycs
Cox5b

Figure 2

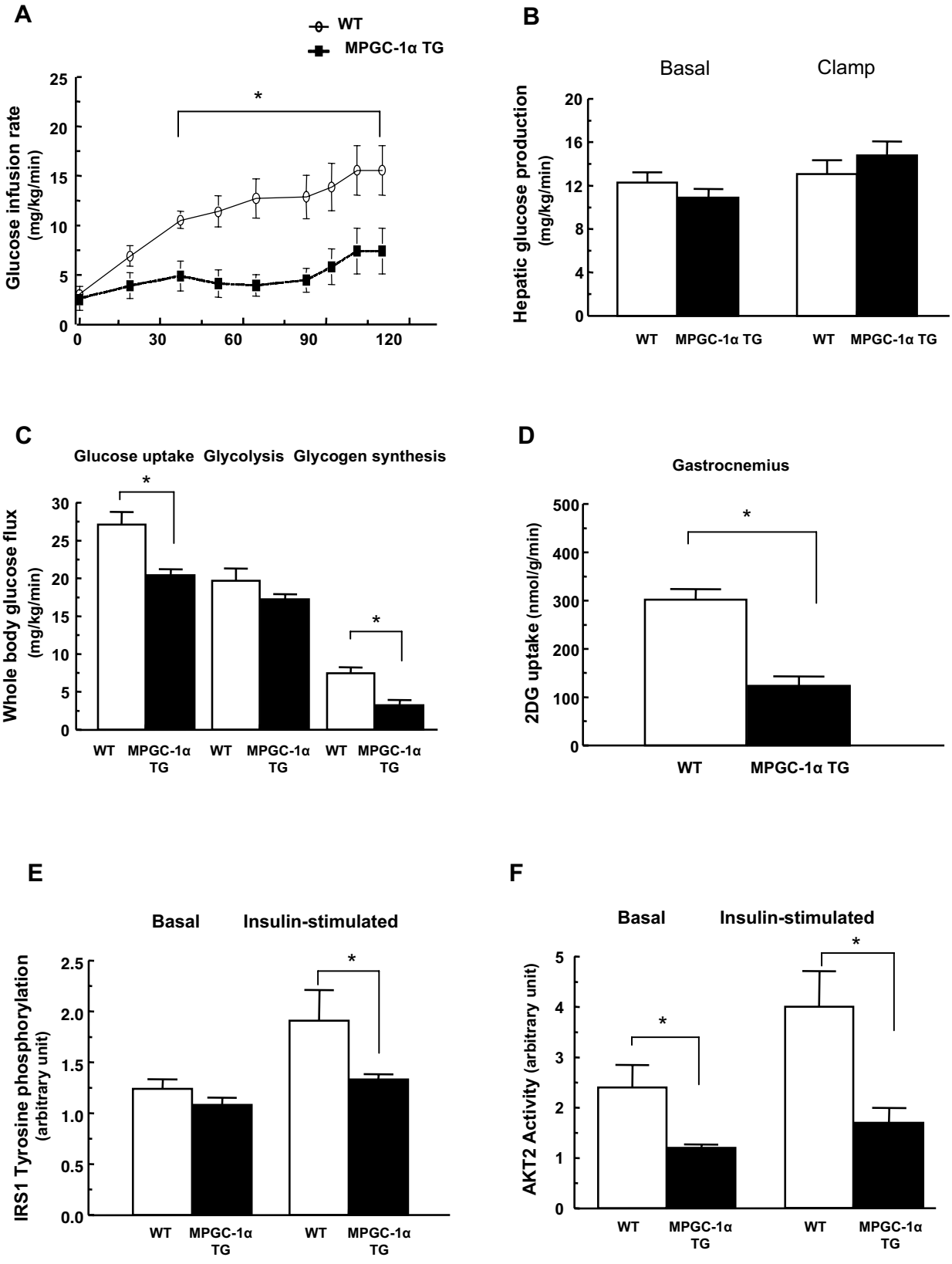
A
WT
MPGC-1α TG
Glucose infusion rate (mg/kg/min)
25
20
15
10
5
0
*
0
30
60
90
120
B
Basal
Clamp
Hepatic glucose production (mg/kg/min)
20
16
12
8
4
0
WT
MPGC-1α TG
WT
MPGC-1α TG
C
Glucose uptake
Glycolysis
Glycogen synthesis
Whole body glucose flux (mg/kg/min)
30
25
20
15
10
5
0
*
*
WT
MPGC-1α TG
WT
MPGC-1α TG
WT
MPGC-1α TG
D
Gastrocnemius
2DG uptake (nmol/g/min)
500
400
300
200
100
0
*
WT
MPGC-1α TG
E
Basal
Insulin-stimulated
IRS1 Tyrosine phosphorylation (arbitrary unit)
2.5
2.0
1.5
1.0
0.5
0.0
*
WT
MPGC-1α TG
WT
MPGC-1α TG
F
Basal
Insulin-stimulated
AKT2 Activity (arbitrary unit)
5
4
3
2
1
0
*
*
WT
MPGC-1α TG
WT
MPGC-1α TG

Figure 3

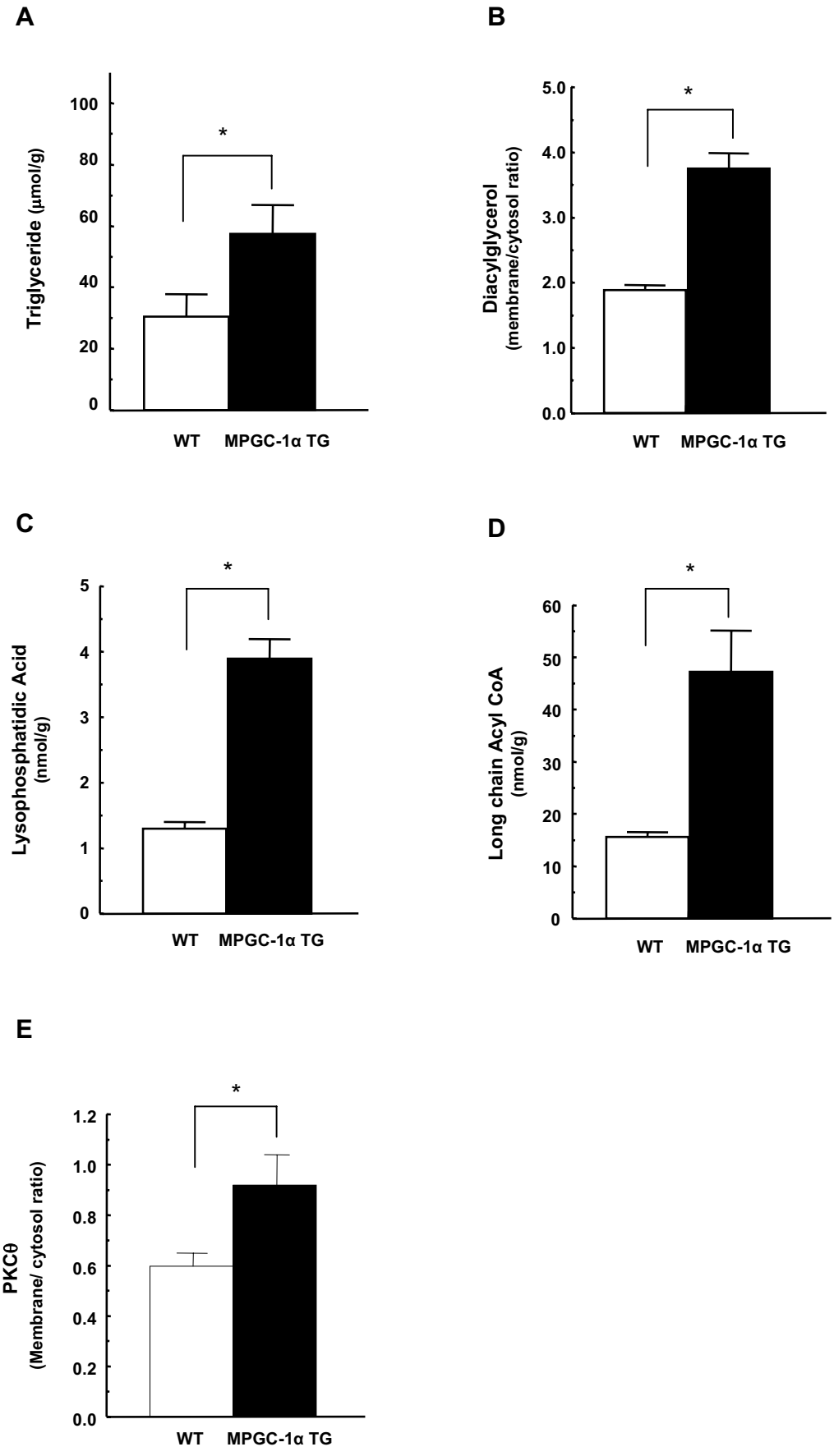
A
Triglyceride (μmol/g)
100
80
60
40
20
0
*
WT
MPGC-1α TG
B
Diacylglycerol
(membrane/cytosol ratio)
5.0
4.0
3.0
2.0
1.0
0.0
*
WT
MPGC-1α TG
C
Lysophosphatidic Acid
(nmol/g)
5
4
3
2
1
0
*
WT
MPGC-1α TG
D
Long chain Acyl CoA
(nmol/g)
60
50
40
30
20
10
0
*
WT
MPGC-1α TG
E
PKCθ
(Membrane/ cytosol ratio)
1.2
1.0
0.8
0.6
0.4
0.2
0.0
*
WT
MPGC-1α TG

Figure 4

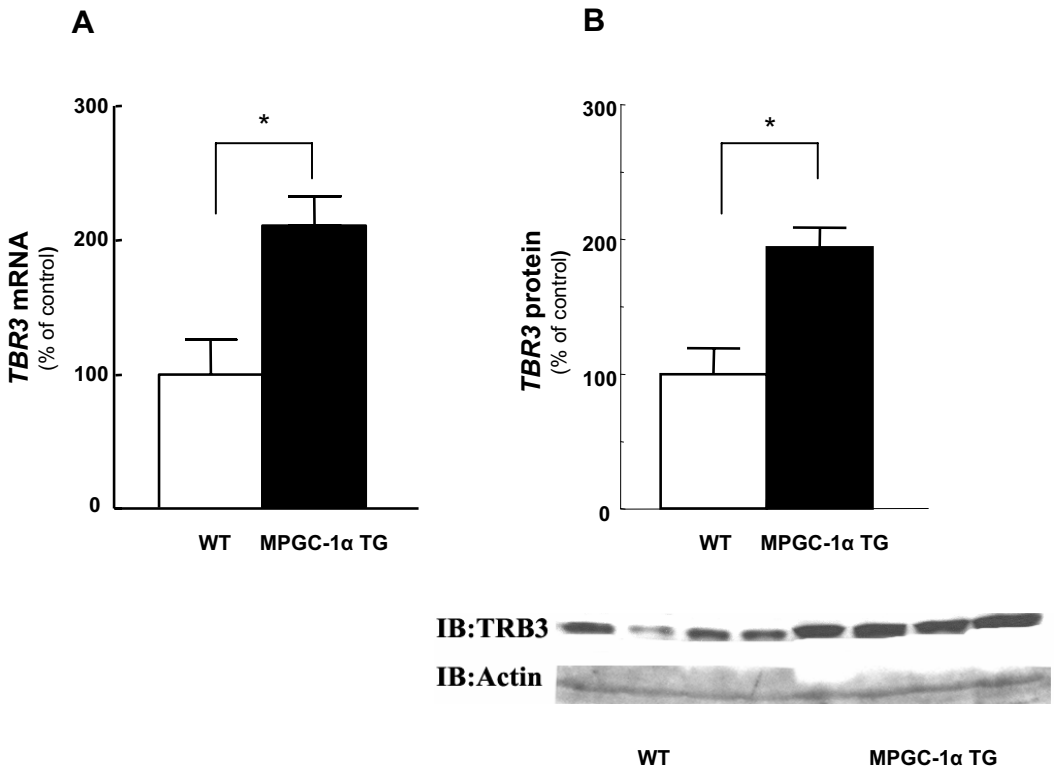
A
B
300
200
100
0
*
TBR3 mRNA
(% of control)
TBR3 protein
(% of control)
WT
MPGC-1α TG
IB:TRB3
IB:Actin
WT
MPGC-1α TG

Figure 5

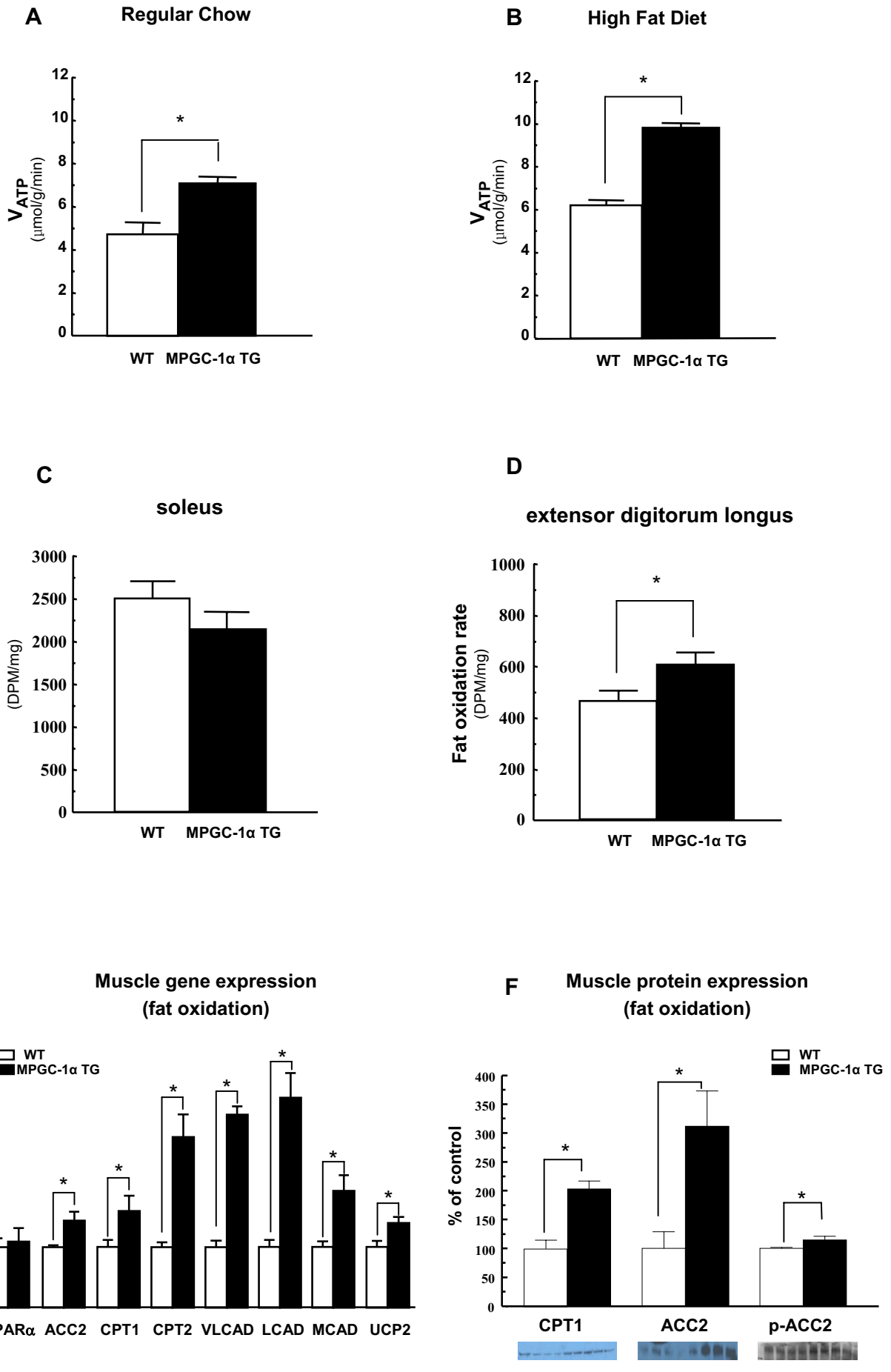
A
Regular Chow
V_{ATP} (μmol/g/min)
WT
MPGC-1α TG
B
High Fat Diet
C
soleus
Fat oxidation rate (DPM/mg)
D
extensor digitorum longus
E
Muscle gene expression (fat oxidation)
% of control
PPARα
ACC2
CPT1
CPT2
VLCAD
LCAD
MCAD
UCP2
F
Muscle protein expression (fat oxidation)
CPT1
ACC2
p-ACC2

Figure 6

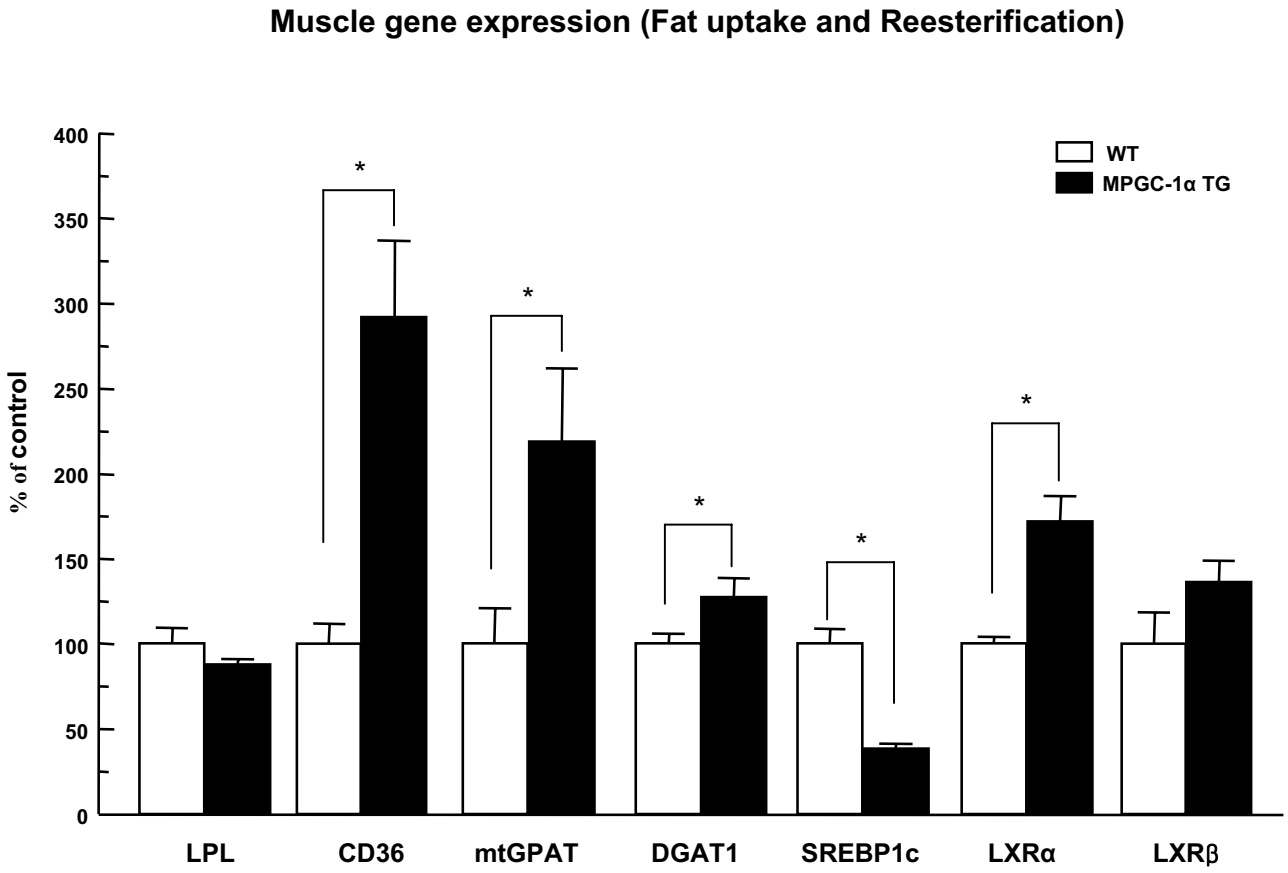
Muscle gene expression (Fat uptake and Reesterification)
WT
MPGC-1α TG
% of control
400
350
300
250
200
150
100
50
0
*
*
*
*
*
LPL
CD36
mtGPAT
DGAT1
SREBP1c
LXRα
LXRβ